Supporting information

Tunable Heteroassembly of 2D CoNi LDH and Ti_3C_2 Nanosheets with Enhanced Electrocatalytic Activity for Oxygen Evolution

Xueyi Lu,[a,‡] Lulu Jia,[b,‡] Minchen Hou,[a] Xuemin Wu,[a] Chang Ni,[a]

Gaofei Xiao,[a,*] Renzhi Ma,[b,*], and Xia Lu[a,*]

[a]School of Materials, Sun Yat-sen University, Shenzhen 518107, P. R. China

[b]Research Center for Materials Nanoarchitectonics, National Institute for Materials Science, Namiki 1-1, Tsukuba 305-0044, Japan

[‡]These authors contribute equally to this work.

E-mails: xiaogf@mail.sysu.edu.cn; MA.Renzhi@nims.go.jp; luxia3@mail.sysu.edu.cn

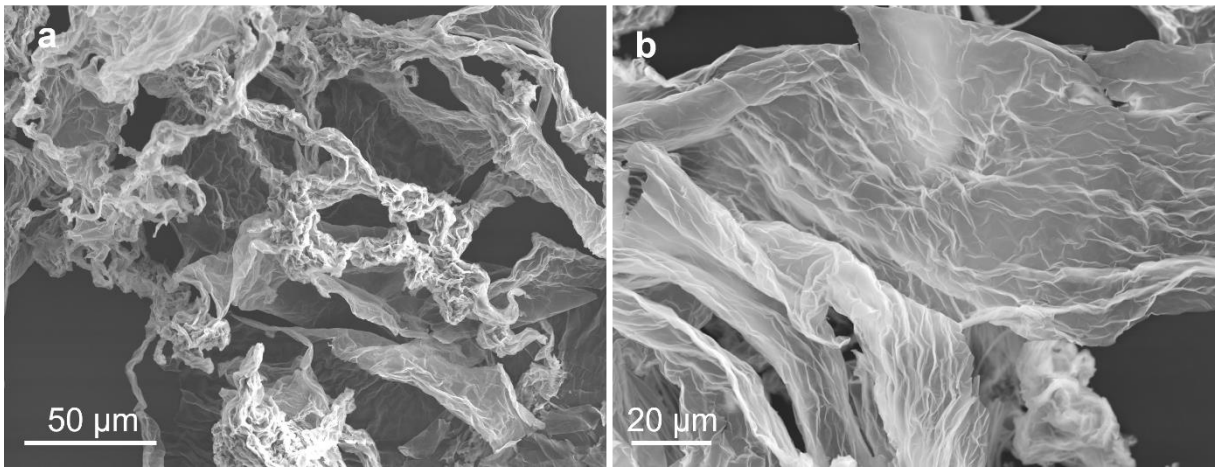

Figure S1. SEM images of CoNi LDH nanosheets after freeze drying.

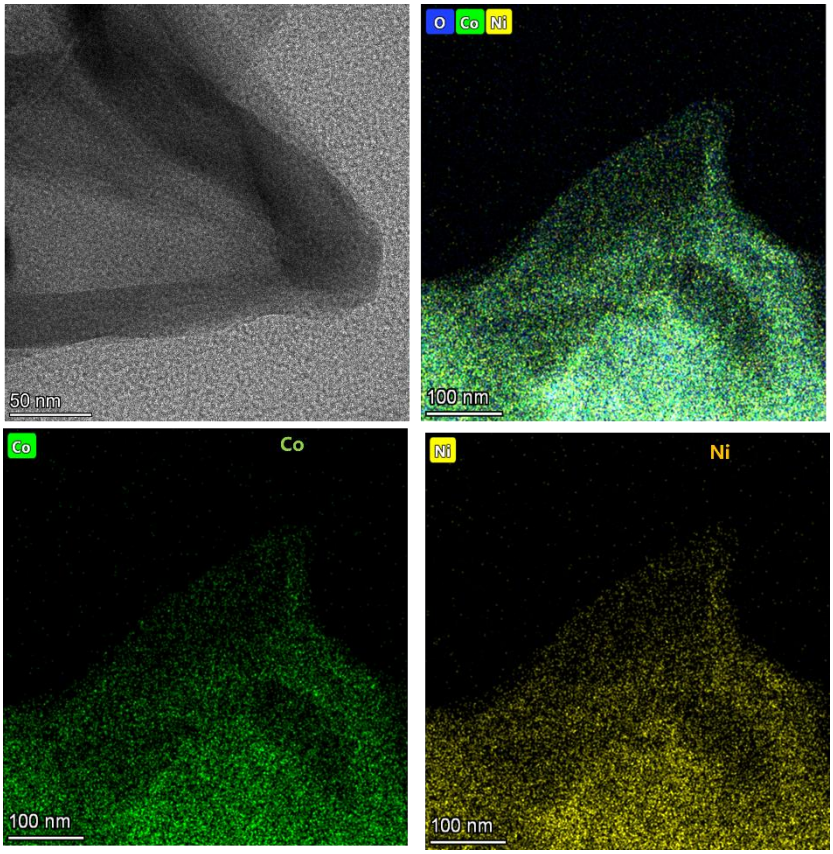

Figure S2. TEM image and elemental mappings of CoNi LDH nanosheets after exfoliation.

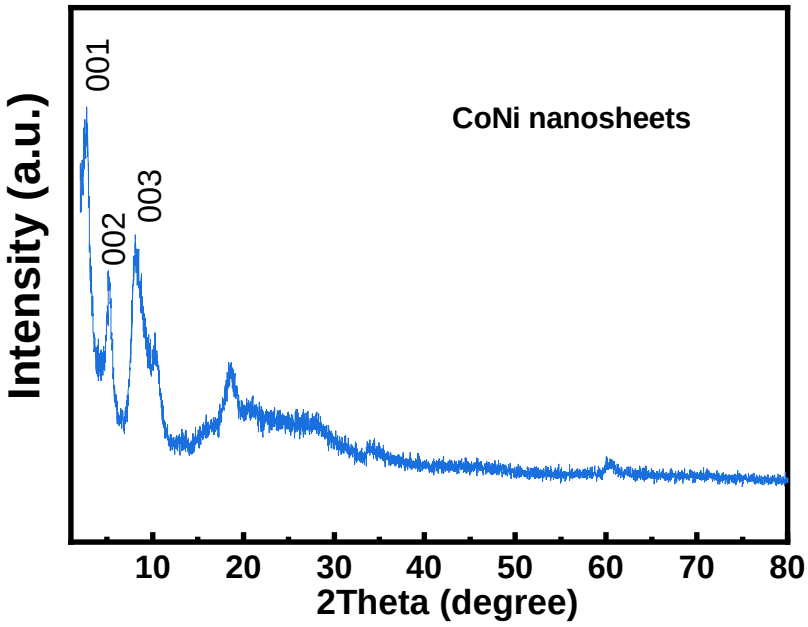

Figure S3. XRD pattern of CoNi LDH nanosheets after freeze drying.

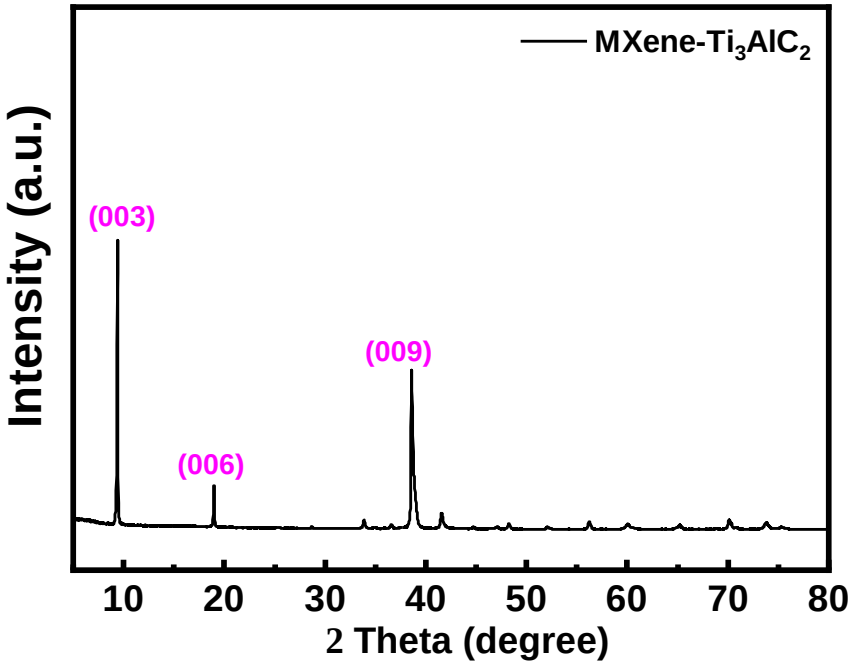

Figure S4. XRD pattern of the multilayered Ti_3AlC_2 MAX.

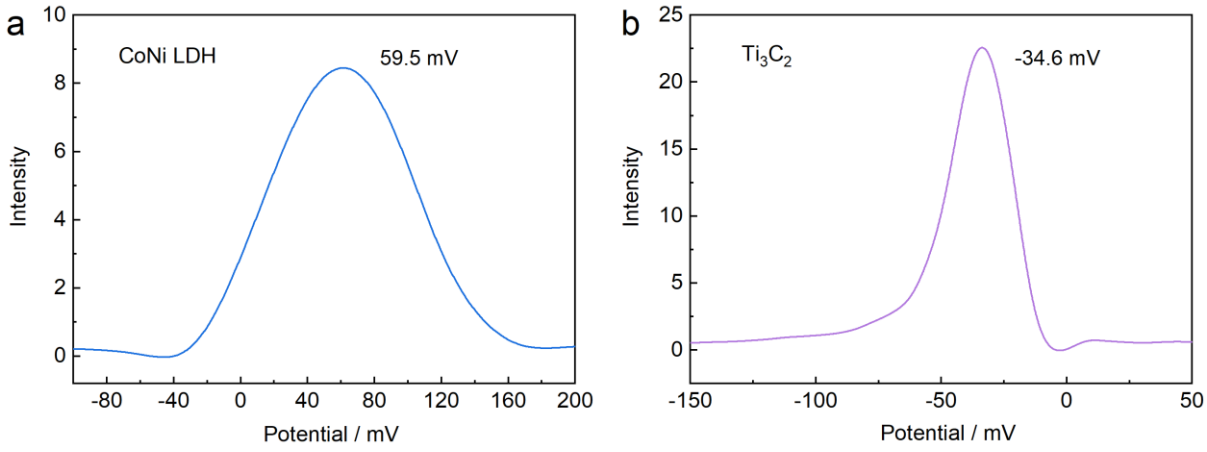

Figure S5. Zeta potential profiles of CoNi LDH and Ti_3C_2 nanosheet dispersion.

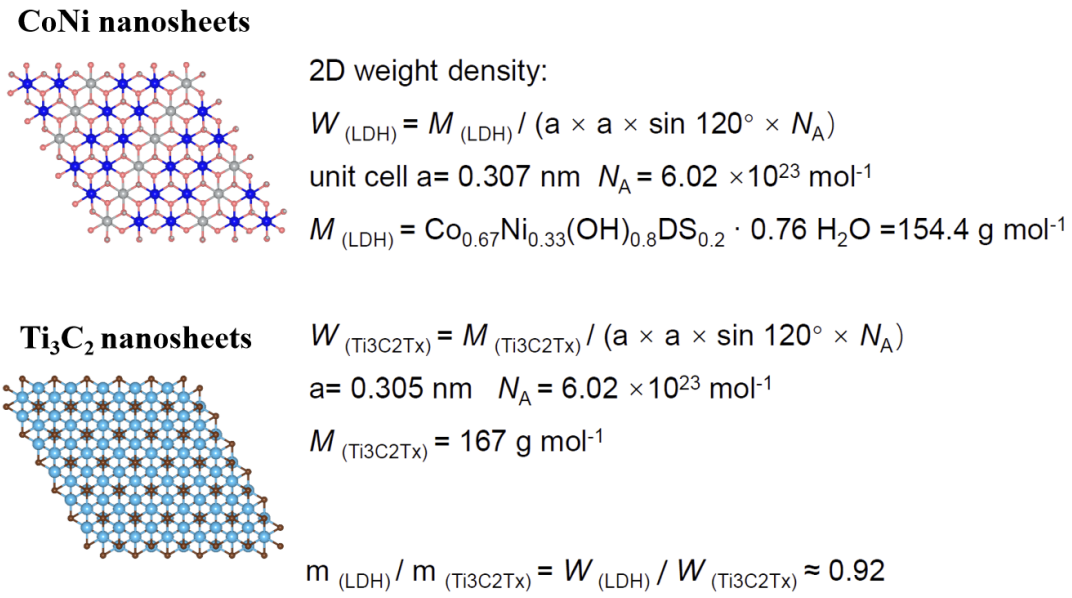

Figure S6. Crystal structure of monolayer CoNi LDH and Ti_3C_2 nanosheets and the area match model for design of the heterostructures.

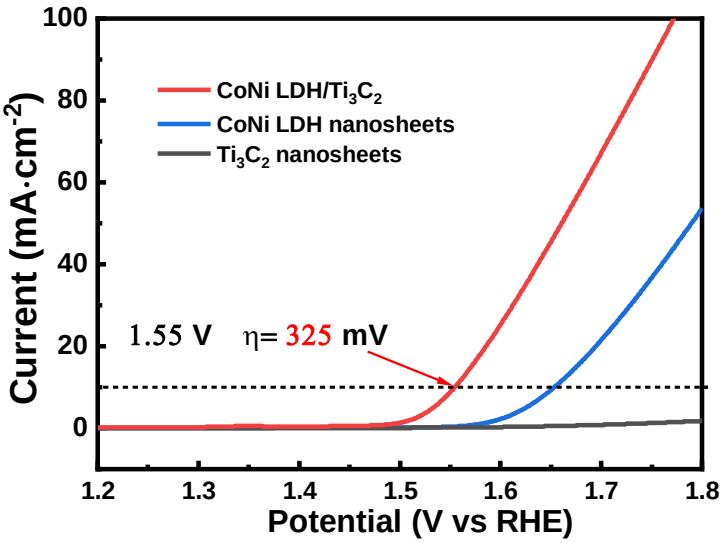

Figure S7. LSV curves for CoNi LDH, Ti_3C_2 nanosheets and CoNi LDH/Ti_3C_2 materials.

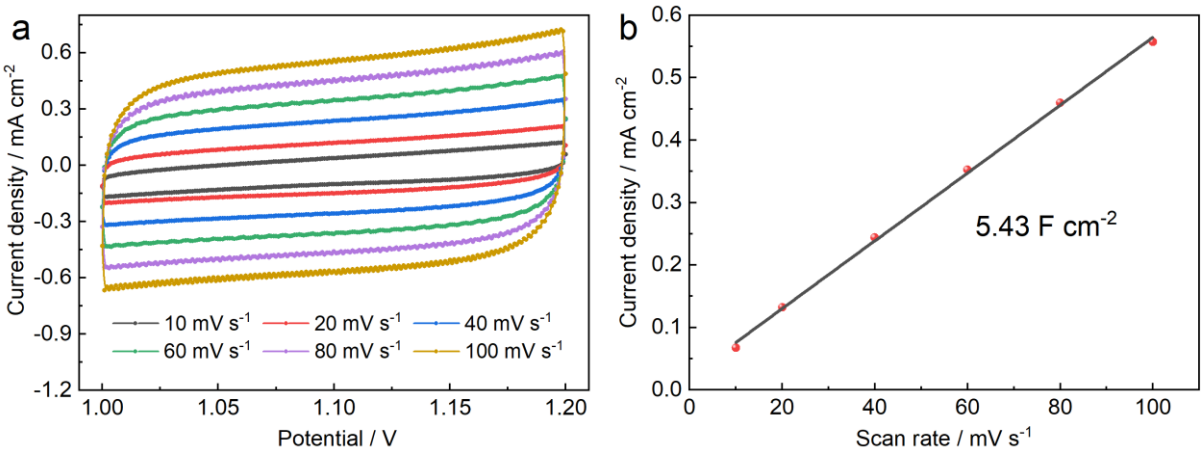

Figure S8. CV profiles of CoNi LDH/Ti_3C_2 at various scan rates and the capacitive currents at 1.1 V plotted as a function of scan rate.

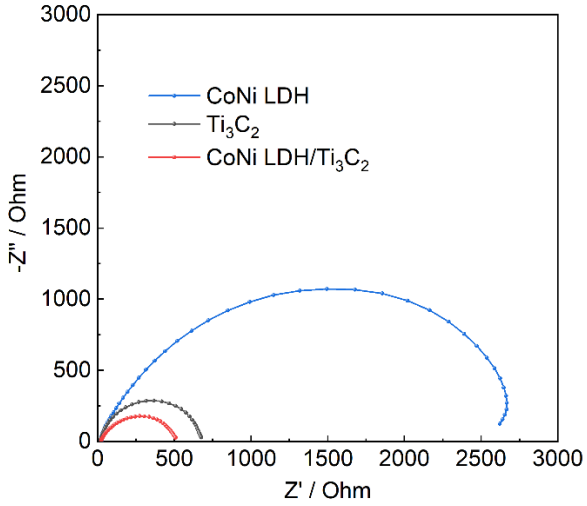

Figure S9. EIS spectra of CoNi LDH, Ti_3C_2 and CoNi LDH/Ti_3C_2 superlattice heterostructures.

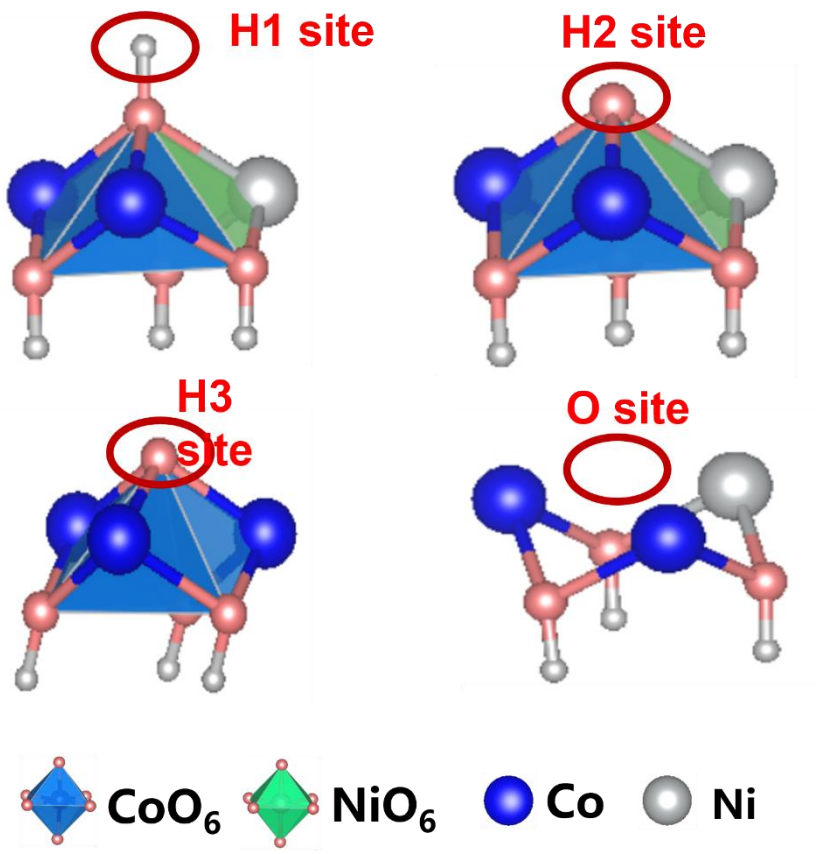

Figure S10. Different active site positions at the CoNi LDH/Ti_3C_2 interface.

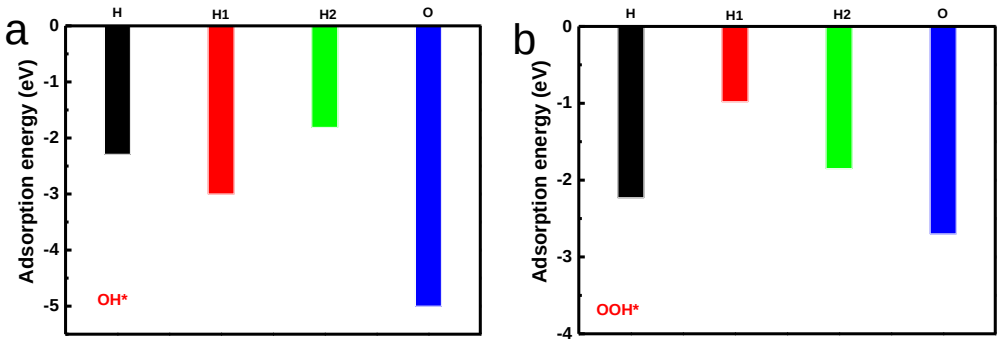

Figure S11. Adsorption energies of different active sites for the intermediates (OH* and OOH) of the OER reaction.

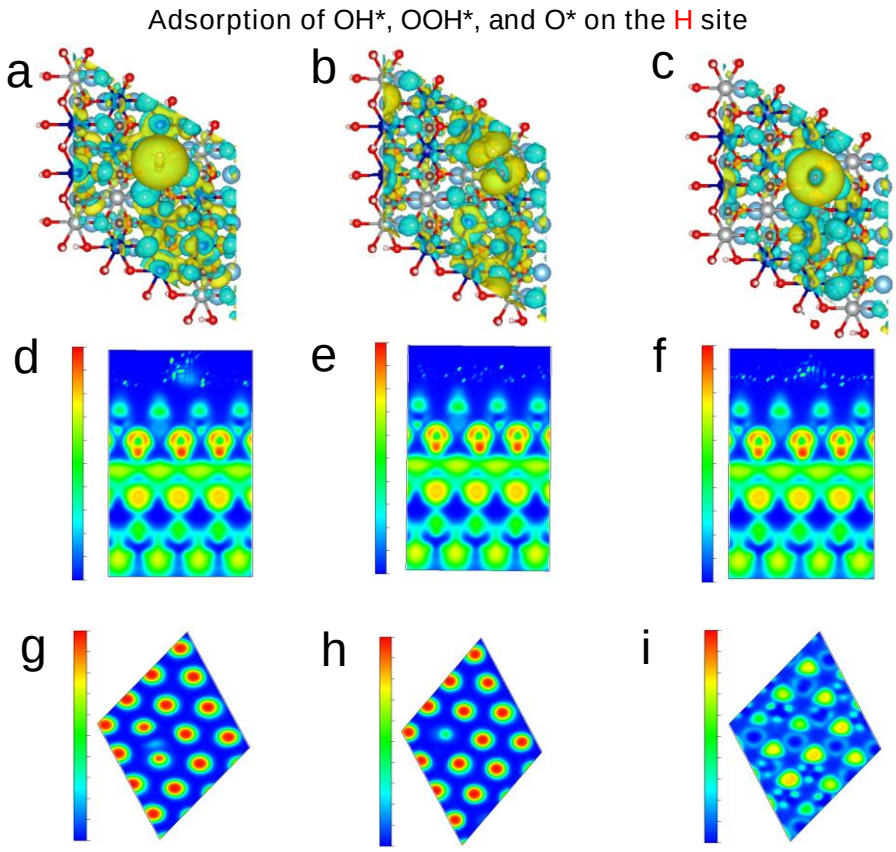

Figure S12. Electron localization function (a-c) and charge density difference (d-i) diagrams for the adsorption of OH* (a, d, f), OOH* (b, e, h), and O* (c, f, i) on the H site.

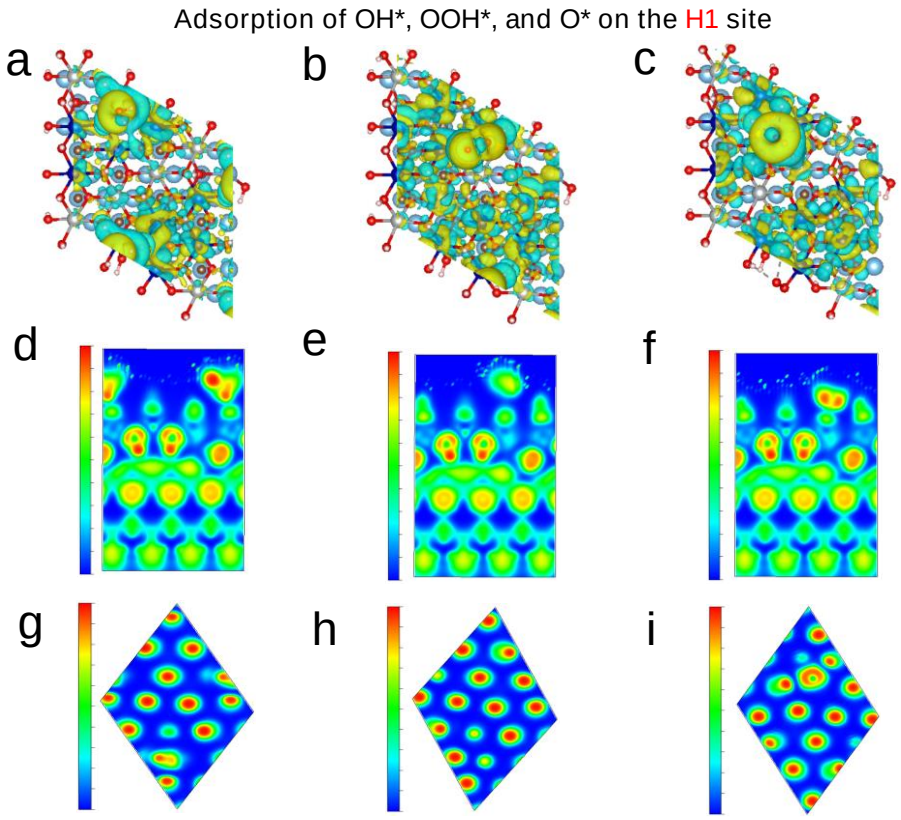

Figure S13. Electron localization function (a-c) and charge density difference (d-i) diagrams for the adsorption of OH* (a, d, f), OOH*(b, e, h), and O*(c, f, i) on the H1 site.

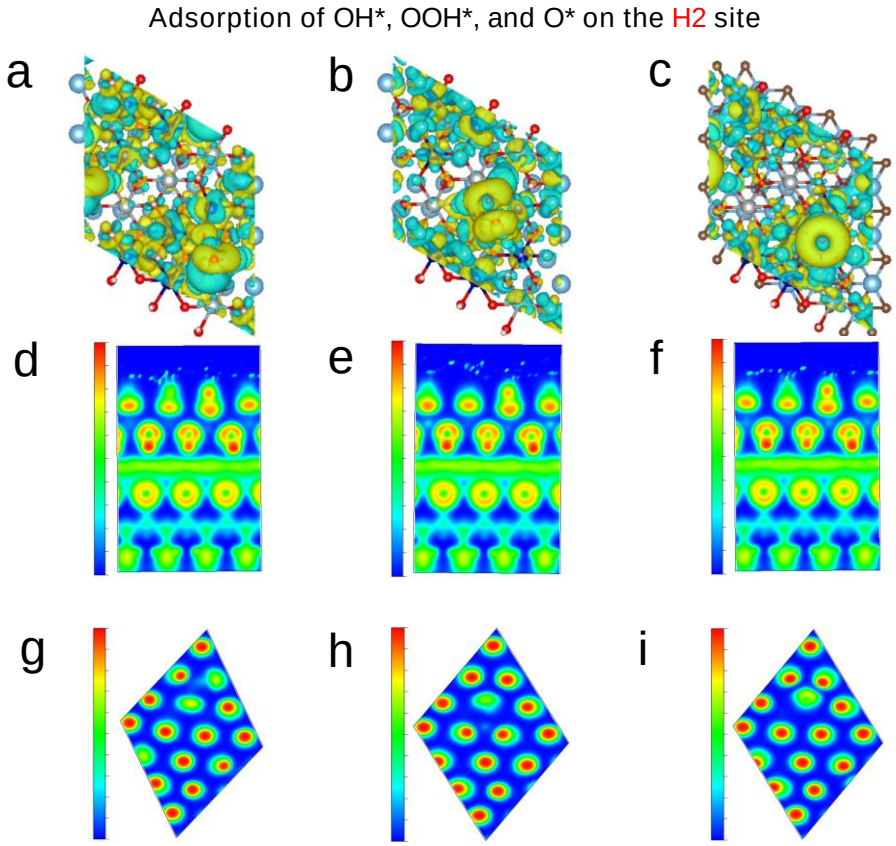

Figure S14. Electron localization function (a-c) and charge density difference (d-i) diagrams for the adsorption of OH* (a, d, f), OOH* (b, e, h), and O* (c, f, i) on the H2 site.

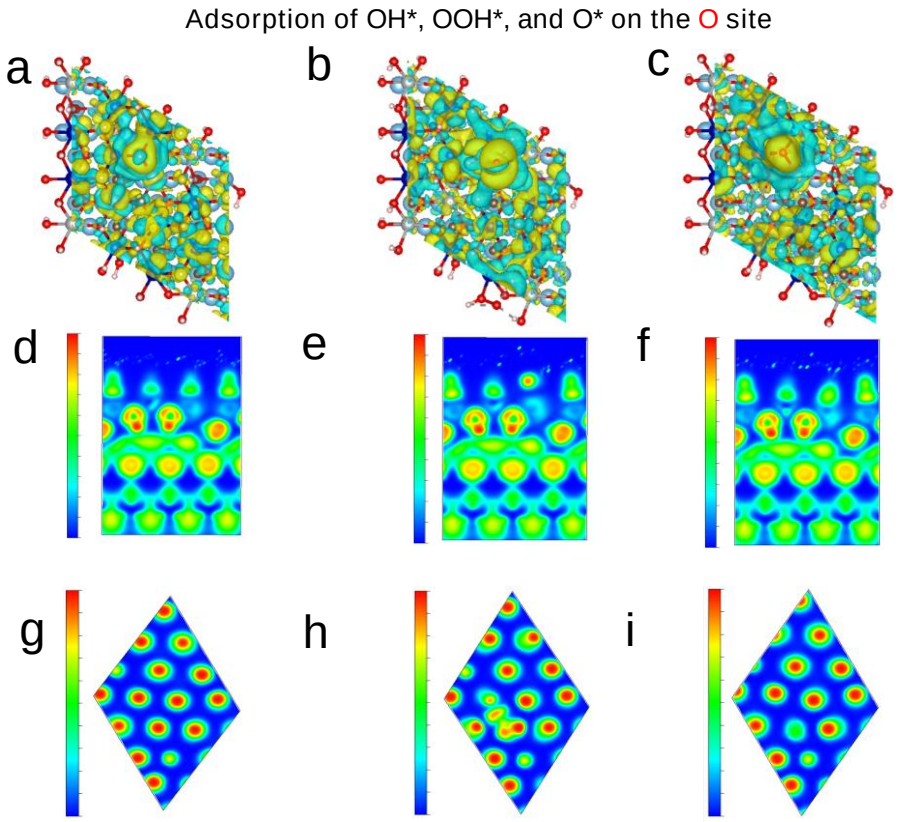

Figure S15. Electron localization function (a-c) and charge density difference (d-i) diagrams for the adsorption of OH* (a, d, f), OOH* (b, e, h), and O* (c, f, i) on the O site.